On the Competition between Water, Sodium Ions, and Spermine in Binding to DNA: A Molecular Dynamics Computer Simulation Study

Nikolay Korolev, Alexander P. Lyubartsev, Aatto Laaksonen, and Lars Nordenskiöld

Division of Physical Chemistry, Arrhenius Laboratory, Stockholm University, S 106 91 Stockholm, Sweden

ABSTRACT The interaction of DNA with the polyamine spermine^{4+} (Spm^{4+}), sodium ions, and water molecules has been studied using molecular dynamics computer simulations in a system modeling a DNA crystal. The simulation model consisted of three B-DNA decamers in a periodic hexagonal cell, containing 1200 water molecules, 8 Spm^{4+}, 32 Na$^+$, and 4 Cl$^-$ ions. The present paper gives a more detailed account of a recently published report of this system and compares results on this mixed Spm^{4+}/Na$^+$-cation system with an molecular dynamics simulation carried out for the same DNA decamer under similar conditions with only sodium counterions (Korolev et al., 2001, *J. Mol. Biol.* 308:907). The presence of Spm^{4+} makes significant influence on the DNA hydration and on the interaction of the sodium ions with DNA. Spermine pushes water molecules out of the minor groove, whereas Na$^+$ attracts and organizes water around DNA. The major binding site of the Spm^{4+} amino groups and the Na$^+$ ions is the phosphate group of DNA. The flexible polyamine spermine displays a high presence in the minor groove but does not form long-lived and structurally defined complexes. Sodium ions compete with Spm^{4+} for binding to the DNA bases in the minor groove. Sodium ions also have several strong binding sites in the major groove. The ability of water molecules, Spm^{4+}, and Na$^+$ to modulate the local structure of the DNA double helix is discussed.

INTRODUCTION

The delicate interplay between the conformational structure of DNA, its hydration, and interactions with various ligands, including mobile counterions, has recently become an object of extensive interdisciplinary studies. Results obtained by experimental (x-ray crystallography, nuclear magnetic resonance (NMR) spectroscopy, fluorescence depolarization) and computational methods are in general mutual agreement concerning the structure and dynamics of the DNA double helix and solvent (water) molecules surrounding DNA oligomers and polymers. However, the participation and specific role of counterions in the modulation of DNA structure and perturbation of the solvation shell around DNA have been much debated in recent literature (McConnell and Beveridge, 2000; Williams and Maher, 2000; Hud and Polak, 2001; Howerton et al., 2001 and references cited therein). Williams and co-workers (McFail-Isom et al., 1999) proposed an idea that water molecules can partially be substituted by monovalent cations in the solvation shells of B-DNA in the crystals of the most frequently studied DNA sequence, the Drew-Dickerson-dodecamer (DDD), d(CGCGAATTCGCG)$_2$ (Drew and Dickerson, 1981). Such interpretation of the x-ray crystallography data is supported by results obtained in several NMR (Halle and Denisov, 1998; Hud et al., 1999; Denisov and Halle, 2000)

and MD simulation studies (Beveridge and McConnell, 2000; Feig and Pettitt, 1999a; Lyubartsev and Laaksonen, 1998; Bonvin, 2000; Young et al., 1997; Hamelberg et al., 2000, 2001) of nucleic acid oligomers in aqueous environment. Williams and coworkers (McFail-Isom et al., 1999; Williams and Maher, 2000; Sines et al., 2000) further proposed that dynamic and sequence-specific variation of the density of ions around electronegative groups of DNA, plays an important role in modulation of certain features of the DNA double helical structure such as the groove width and bending. They have also suggested that this phenomenon could contribute to the structural transition behavior of DNA and to protein-DNA recognition and binding. However, their interpretation of the x-ray diffraction data has been the subject of criticism from other x-ray crystallography groups (Chiu et al., 1999; Tereshko et al., 1999a,b; Egli et al., 1998; Vlieghe et al., 1999). An example of this is the crystallization and structural analysis of the DDD duplex that was repeated to atomic resolution by Dickerson and coworkers (Chiu et al., 1999). The authors (Chiu et al., 1999) showed that the interpretation advocating the presence of counterions in the spine of hydration (Shui et al., 1998a; McFail-Isom et al., 1999) most probably was incorrect. Moreover, chemical analysis revealed that monovalent cations are simply absent in the DNA crystal of this study (the amount of Mg^{2+} found in the analysis was more than enough for neutralization of the DNA charge). Based on their results, Dickerson and co-workers also criticized the major implications forwarded by McFail-Isom et al. (1999) concerning the role of counterions in modulation of DNA structure and dynamics as well as in DNA-protein interactions.

Another closely related issue is that none of the high-resolution x-ray diffraction studies has been able to locate all (not even a major part of) the cations neutralizing the total charge of the DNA phosphate groups in the crystallo-

graphic cell. The most successful identification of ions refers to the localization of hydrated Mg^{2+} or Ca^{2+} (Soler-Lopez et al., 1999, 2000). However, additional ionic species, present in the crystallization solutions of DNA oligomers, such as monovalent cations and the highly positively charged polyamine spermine^{4+} (Spm^{4+}; H$_3$N$^+$-(CH$_2$)$_3$-NH$_2^+$-(CH$_2$)$_4$-NH$_2^+$-(CH$_2$)$_3$-NH$_3^+$), have largely escaped detection in the x-ray diffraction studies made on crystals grown from these solutions. The structurally undefined and mobile character of their interactions with DNA can explain the invisibility of the monovalent (M$^+$) ions like Na$^+$ or K$^+$. The failure to locate spermine in B-DNA crystals is, however, rather unexpected. According to polyelectrolyte theories, this highly charged ligand should be more strongly absorbed by DNA than cations with lower charges (M$^+$ or Mg^{2+}). This situation is unfortunate because the understanding of spermine-B-DNA interactions is important, not only because of its role as a crystallizing agent, but also because this polyamine is present in millimolar concentrations in all eukaryotic cells and plays a significant, albeit not yet clearly resolved, role in biological reactions involving DNA and RNA (Cohen, 1998).

In the original x-ray work of Drew and Dickerson (1981) on the DDD crystal, it was concluded that one single spermine molecule is bound to DNA across the major groove near the (CGCG)$_2$ sequence. Later, the authors refrained from this interpretation and in a recent high-resolution study they could not find any Spm^{4+} molecules in the DDD crystal (Chiu et al., 1999). In another study of the DDD crystal, one partial Spm^{4+} molecule was identified near the edge of the crystallographic unit (Shui et al., 1998b,a). In this work, a high concentration of spermine salt was used compared with the other B-DNA crystal preparations.

It should be noted that crystallographic studies of A- and Z-forms of DNA have succeeded in locating spermine ions close to the DNA phosphates (Tippin and Sundaralingam, 1997; Egli et al., 1998; Bancroft et al., 1994). Compared with B-DNA crystals, A- and Z-DNA crystals generally give better resolution in x-ray diffraction because DNA is more densely packed and these structural forms of DNA are more rigid. Despite this fact, the localization of spermine molecules was not easy even in these A- and Z-DNA crystals (Bancroft et al., 1994). The absence, or difficulty to locate spermine in the B-DNA crystal studies has usually been rationalized by a nonregular and quite mobile interaction of this polyamine with DNA or by simply assuming that it is absent in the crystals.

Molecular modeling of spermine-DNA interactions has shown that several of the most favorable binding conformations of Spm^{4+} have relatively small differences in energy (Zakrzewska and Pullman, 1986). In addition, in early molecular dynamics (MD) simulations, Spm^{4+} was found to destabilize the B-DNA double helix leading to speculations about possible initial steps in a Spm^{4+}-induced B-Z transition (Haworth et al., 1992). Both molecular modeling and
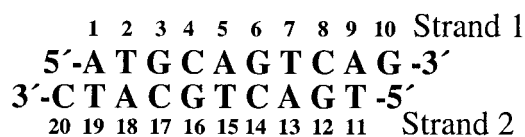
FIGURE 1 DNA sequence studied in this work. Note that the sequence has "sticky" ends, which means that unpaired bases of the 3′-terminals are connected to the mirror images of the decamer along z direction.

experimental studies have been carried out in attempt to confirm the sequence (to the CG/CG dinucleotide step) and groove (in the major groove of B-DNA) specific Spm^{4+} binding (Feuerstein et al., 1986, 1990; Yuki et al., 1996; Shamma and Haworth, 1999). These simulations, however, were performed for considerably simplified systems without explicit solvent molecules with no charge balance in the simulation cell and for rigid structure of DNA. The simulations were also rather short (0.8–1.6 ns in the work of Yuki et al. (1996) or 1 ns in the paper of Shamma and Haworth (1999)).

Recently, we published a combined grand canonical Monte Carlo (GCMC) and molecular dynamics computer simulation study of the Spm/Na B-DNA system (Korolev et al., 2001). GCMC calculations were used to calculate the distribution of counterions of different valencies between the equilibrating solvent and the DNA crystal under conditions mimicking the crystal-growing protocols of several x-ray diffraction studies. The GCMC simulations showed that the composition of ions neutralizing the charge of DNA could vary in a broad range depending on the conditions. In general, Spm^{4+} will, however, be accumulated in the crystals if it is present in the crystallizing solution. A 6-ns MD simulation of DNA with the base sequence shown in Fig. 1, consisting of three DNA double helix decamers in a periodic hexagonal cell, containing 1200 water molecules, 8 Spm^{4+}, 32 Na$^+$, and 4 Cl$^-$ ions was carried out. The composition of the species in the simulation cell corresponds to that of real crystals studied by x-ray diffraction crystallography (Korolev et al., 2001). Based on the simulation results, it appears that the flexible polyamine molecule has several binding modes, interacting in fairly irregular manner with different sites on DNA and showing no regular ordering in the DNA crystals. This can explain why Spm^{4+} is not detected in x-ray studies.

The account of the MD simulation in our previous publication was limited and focused on the presentation of the GCMC results and on the MD data describing interaction of spermine with DNA. However, a wealth of additional information can be obtained from the simulation, particularly regarding the distribution of sodium ions and water around DNA. The present work gives a more complete analysis of the MD simulation, partially presented in our previous work, now focusing on the details of Na$^+$ and water interaction with DNA and how this is affected by the presence of spermine. We present more details about the spermine in-

teraction with DNA with a particular emphasis on the competition of the polyamine with Na^+ and water. To illustrate the effect of the presence of spermine on the hydration of DNA and on the association of Na^+, we have also performed a new simulation on a completely analogous system with three decamers containing no spermine molecules but with Na^+ as the only counterion. Furthermore, on the basis of new analyses we make some comparison with a previous simulation, (Lyubartsev and Laaksonen, 1998) on a system consisting of a single DNA decamer but with a somewhat higher water content than in the new Na-DNA simulation with three decamers (25 compared with 20 H_2O per DNA nucleotide, respectively). Based on the MD simulation results we also discuss the ability of Spm^{4+}, Na^+, and water molecules to modulate the local structure of the DNA double helix.

COMPUTATIONAL DETAILS

A hexagonal simulation cell with periodic boundary conditions imposed in all directions was filled with three identical B-DNA decamers (see the base sequence in Fig. 1), carrying a total negative charge of -60. To neutralize the DNA, the simulation cell contained 8 Spm^{4+} and 32 Na^+ ions together with 4 Cl^- coions. In addition, 1200 water molecules, represented by the flexible simple point charge water model by Toukan and Rahman (1985) were added to the system (this system is abbreviated Spm/Na). To compare the influence of Spm^{4+} and Na^+ on DNA structure and dynamics, we performed an additional MD simulation (abbreviated as Na-3DNA) with Na^+ as the single counterion. In the Na-3DNA run, the simulated cell was analogous to that of the Spm/Na system, i.e., a hexagonal cell containing 3 DNA decamers, 1200 H_2O, 64 Na^+, and 4 Cl^- ions. Furthermore, by performing new analyses, we have made comparison with our previous MD simulation (Lyubartsev and Laaksonen, 1998) consisting of a single DNA decamer of the same base sequence that contained 20 Na^+, 500 water molecules with no chlorine co-ions in a cubic simulation box (abbreviated as Na-1DNA). The major difference between the Na-3DNA and Na-1DNA systems, except for the number of decamers in the cell, is that the relative amount of water molecules in the Na-1DNA simulation is somewhat higher than in the Na-3DNA system (25 and 20 H_2O per DNA nucleotide, respectively).

The CHARMM (version 2.2) force field (MacKerell et al., 1995) was used to model both the DNA system and the spermine molecules. Another force field, often used for molecular dynamics simulations of DNA is AMBER (Cornell et al., 1995). Usage of different force fields may give somewhat different DNA structures. The version of CHARMM used in this work is slightly favorable to the A-form (Feig and Pettitt, 1998). It was shown, however, that the hydration structure and ion distribution around DNA is very similar in AMBER and CHARMM simulations (Feig and Pettitt, 1999a,b). Our previous simulations of a periodic

DNA fragment within the same model and periodical boundary conditions have shown stable, B-form like DNA structures (Lyubartsev and Laaksonen, 1998). Note also, that DNA periodicity along the z axis fixes the helical twist of DNA (10 base pairs per turn) and inhibits major bending of DNA. Whereas these effects may in principle affect the ion association, we expect the influence to be small because the imposed periodicity leaves enough freedom for local motions of DNA structure.

The long-range electrostatic interactions were treated by the Ewald summation method. Nóse-Hoover thermostats and barostats were applied to keep the temperature and pressure at around 300 K and 1 atm. The pressure was controlled separately in directions parallel and perpendicular to DNA-helix. A double time step algorithm by (Tuckerman et al., 1992), with short time step of 0.2 fs for fast intramolecular vibrations and the short-range part (within 5 Å) of intermolecular interactions and long time step of 2 fs for longer-range interactions were implemented. The simulation software used is the M.Dyna*Mix* package by Lyubartsev and Laaksonen (2000). All the simulations were carried out on a cluster of dual processor Intel Pentium III PC running Linux as operating system. More details on the computational algorithm are given in our previous MD simulation studies (Lyubartsev and Laaksonen, 1998, 1999, 2000).

In the beginning of the Spm/Na simulation, the spermine molecules were positioned between DNA molecules at equal distance from each DNA with water molecules and small ions filling the remaining space. A 100-ps run, at constant volume and fixed DNA and spermine atom coordinates was initially performed, to allow water molecules to form hydration shells around DNA and ions. After that, all atoms were released, and the constant-pressure molecular dynamics algorithm started. An additional 200-ps run was carried out to allow all atoms to equilibrate, and then a 6-ns production run was performed, during which all distribution functions and statistical averages were calculated. For the Na-3DNA simulation, an initial configuration was generated from a snapshot of the Spm/Na system by removing spermine hydrogen and carbon atoms and replacing N^+-atoms for Na^+. After a constant volume equilibration of the system for 100 ps, constant pressure and temperature MD simulation run was performed with the trajectories collected from 0.2 to 3.2 ns.

RESULTS AND DISCUSSION

General properties of the Spm/Na, Na-3DNA, and Na-1DNA systems

In Table 1 the presented data show some general properties (box size, density, concentrations, and diffusion coefficients) obtained from the two MD simulations consisting of three identical DNA decamers but with different counterion

TABLE 1 Properties of the Spm/Na, Na-3DNA, and Na-1DNA systems

System	Cell dimension and geometry, Å	Density, g/cm^3	Box volume, nm^3	Species concentration, M	Diffusion parameters: $D \times 10^{10}$, m/c^2 (R, Å)*	
Spm/Na	$44.5 \times 38.5 \times 31.8$ Hexagonal	1.298	54.4	36.62 (H_2O)	5.0 (16.4)	H_2O
				0.244 (Spm^{4+})	0.12 (2.8)	Spm^{4+}
				0.977 (Na^+)	1.4 (9.15)	Na^+
				0.122 (Cl^-)	2.0 (10.5)	Cl^-
Na-3DNA	$44.2 \times 38.3 \times 30.85$ Hexagonal	1.328	51.9	38.40 (H_2O)	4.6 (17.1)	H_2O
				2.045 (Na^+)	1.3 (9.5)	Na^+
				0.128 (Cl^-)	2.5 (10.5)	Cl^-
Na-1DNA	$24.7 \times 24.7 \times 33.7$ Rectangular	1.262	20.6	40.36 (H_2O)	$\approx$10 (23.1)	H_2O
				1.624 (Na^+)	1.3 (9.5)	Na^+

*D is diffusion coefficient; R is mean displacement calculated for 1 ns.

mixtures. In addition, we also present the same information from our previous simulation (Lyubartsev and Laaksonen, 1998) consisting of a single DNA decamer. The distance between axes of neighboring DNA molecules was ~25 Å and fluctuated no more than 1 Å during the course of the simulations. In the two simulations with three DNA decamers in the cell we observed stable, B-form like DNA structures, with root mean square (RMS) deviations similar to that observed earlier (Lyubartsev and Laaksonen, 1998) for the Na-1DNA system. We note that in our simulation setup the B-form was stabilized due to topological constraints (10 base pairs per turn) arising from the periodic boundary conditions. It may be noted that the water content, measured as the number of water molecules per nucleotide, is the same (20) for the systems with three decamers in the simulation cell. Furthermore, the number of positive counterions (N^+ from spermine and/or Na^+) as well as the number of co-ions is the same in the Spm/Na and Na-3DNA systems. Consequently, due to the presence of bulky spermine molecules, the volume is larger in the Spm/Na system.

Water, Na^+, and Cl^- are very mobile and the trajectories of these species, collected during 3 to 6 ns and averaged over three DNA duplexes should be representative enough for determination of their mobility and binding characteristics, although conclusive statements about statistical error limits require more simulations. Interactions of Spm^{4+} with DNA as well as the Spm^{4+}, water, and Na^+ competitions in the vicinity of the DNA groups were recorded during 6 ns. This may not be enough to obtain properly averaged binding properties but should allow us to describe reasonably well the Spm^{4+} binding in the DNA crystals (see our previous work (Korolev et al., 2001) for more discussion).

The positions and intensities of the first and second maxima of the radial distributions functions (RDF) between the water oxygens as well as the ions (N^+ atoms of spermine and Na^+) with different sites on DNA are collected in Table 2. The occupancies at these sites, as well as the average residence times, are given in Table 3. The occupation numbers were calculated by integrating the RDFs up to the position of the first minimum. Data presented in Tables 2 and 3 were obtained by averaging over all sites of the

given type in the DNA fragment. To describe the site-specific (sequence-dependent) binding of Na^+ to DNA bases we have carried out a separate analysis, summarized in Table 4, giving similar information as that in Tables 2 and 3, but for some selected sites of the decamer. As additional information, the longest single residence times during the 6 ns (for Spm/Na system) or 3 ns (Na-3DNA system) simulation are also reported. We will refer to these tables below in the discussion. In Tables 2 to 4, the parameters calculated for Na^+ and water are given for both systems.

The results of the simulation regarding the solvation and coordination around DNA can be further visualized using three-dimensional spatial distribution functions (SDF). When displaying SDF around a two base-pairs fragment, we have defined the molecular frame from the phosphate coordinates (Lyubartsev and Laaksonen, 1998) using a procedure similar to that by Cheathan and Kollman (1997). The SDFs drawn around the whole decamer were calculated in a frame obtained by the best fit to the original (B-form) DNA conformation. We have also used RDF for presentation and discussion of the results. To illustrate the effect of the presence of spermine on the association of sodium and water with DNA, we will present similar structural (averaged and snapshot DNA structures, RMS values) and binding (SDF, RDF, occupancy) parameters obtained from the Na-3DNA and in some cases also the Na-1DNA simulation.

Summary of the spermine^{4+}-DNA interactions

Analysis of the interaction of spermine^{4+} with the DNA decamer in a crystal environment has already been presented in our previous work (Korolev et al., 2001). Below we list the most essential features of the Spm^{4+} interaction with DNA. 1) The major binding site in DNA for the charged amino groups of Spm^{4+} is the phosphate group (O1P- and O2P-atoms, Table 1 and 2). 2) The long and flexible Spm^{4+} molecules form numerous bridges between neighboring DNA duplexes (mostly, by binding to the phosphate groups), and across the minor and major grooves of each DNA double helix in the simulation cell. 3) Two areas

TABLE 2 Intensities of the first and second maxima and corresponding distances in Å (in parentheses) of the radial distribution functions between oxygen atoms of water, sodium ions, and spermine nitrogen atoms, respectively, and selected sites at DNA

	O_{H2O}	Na^+	$N^+_{terminal}$	$N^+_{central}$
Phosphate oxygen				
O1P				
1st	3.5/3.4 (2.6)	3.8/7.7 (2.3)	7.2–13.0 (2.7)	3.3–4.2 (2.7)
2nd	1.4/1.4 (4.4)	1.7/2.2 (4.6)	1.5–2.2 (4.5–4.8)	1.7–2.2 (4.5–4.8)
O2P				
1st	3.5/3.5 (2.6)	3.2/2.5 (2.3)	2.2–10.0 (2.7)	1.5–3.0 (2.7)
2nd	1.3/1.2 (4.4)	1.8/2.0 (4.6)	1.3–1.8 (4.5–4.6)	0.8–1.5 (4.5–5.0)
Minor groove				
T_{O2}				
1st	0.95/1.15 (2.7)	5.0/0.58 (2.3)	7.0 (2.8)	2.2–7.0 (2.8)
2nd	0.45/0.45 (4.7)	0.8/0.7 (4.8)	0.4–1.0 (5.2–5.5)	0.7–2.0 (4.3–4.5)
C_{O2}				
1st	0.75/0.95 (2.7)	0.1/0.78 (2.5)	3.0 (2.8)	0.3–0.8 (2.8–3.0)
2nd	0.35/0.5 (4.6)	0.8/0.93 (4.5)	5.2 (4.5)	1.5–3.3 (4.5–5.0)
A_{N3}				
1st	1.0/1.0 (2.8)	0.2/0.82 (2.6)	–	–
2nd	0.4/0.5 (4.6)	1.3/1.05 (4.6)	3.5 (5.0)	0.7–1.8 (4.2–5.2)
G_{N3}				
1st	1.1/1.1 (2.8)	0.2/0.0 (2.6)	0–1.0 (2.9)	–
2nd	0.4/– (4.6)	1.0/0.7 (4.8)	0.4–0.5 (4.0–5.5)	0.9–1.8 (6.0–6.2)
Major groove				
A_{N7}				
1st	0.9/0.8 (2.8)	2.5/3.8 (2.6)	–	–
2nd	0.5/1.1 (3.5)	0.6/0.6 (4.7)	1.0 (5.5)	0.4–1.6 (7.0–7.6)
G_{N7}				
1st	1.5/1.1 (2.8)	6.3/11.0 (2.4)	–	–
2nd	0.8/0.75 (6.0)	1.0/0.6 (4.4)	0.2–1.1 (5.0–6.3)	0–1.2 (9.5)
G_{O6}				
1st	1.0/0.7 (3.0)	5.5/7.5 (2.3)	–	–
2nd	0.5/0.45 (5.5)	0.8/0.8 (4.6)	0.3–1.6 (8.0–9.0)	0–0.9 (9.0)
T_{O4}				
1st	1.0/0.85 (2.7)	1.0/2.0 (2.3)	–	–
2nd	0.7/0.6 (4.8)	1.2/1.1 (4.5)	0.3–1.1 (6.5–7.2)	0–0.4 (7.3)
C_{N4}				
1st	1.0/0.95 (3.0)	0/0	–	–
2nd	0.7/0.7 (7.2)	0.9 (4.1)	0.4–1.2 (7.3–7.5)	0.4–1.3 (8.5–8.6)
Sugar				
O4*				
1st	0.8 (2.8)	0.4/0.45 (2.6)	2.0 (2.9)	0–0.4 (3.1)
2nd	0.9 (5.8)	1.1/0.7 (4.7)	0–1.6 (4.6)	0–2.3 (4.8)

For Spm^{4+} nitrogen atoms, data are calculated for both ends N1 and N14 denoted $N^+_{terminal}$ and for N5 and N10 denoted $N^+_{central}$. For the data separated by a slash, the first figure reports the value obtained in the Spm/Na system, the second one is for the Na-3DNA system.

of the minor groove of the decamer show rather significant population of spermine. First, a dense but poorly structured "cloud" of different Spm^{4+} subgroups is found in the A5-C8/G12-T15 region along the minor groove center. Second, a layer of spermine molecules covers sugar-phosphate backbone along the sequence G16-C17-A18 from the side of the minor groove. 4) Spermine^{4+} does not interact with the bases in the major groove of the decamer

Our results on spermine^{4+}-DNA interaction are in agreement with the data of recent experimental studies (Deng et al., 2000; Sy et al., 1999). Bloomfield and co-workers have studied the influence of polyamines (spermine and spermidine) on Raman spectra of various genomic DNA (Deng et al., 2000). In that work, it was shown that the polyamines bind preferentially to the DNA phosphate groups and the changes in the Raman spectra are largely independent of the DNA composition. In another experimental and molecular modeling study, it has been shown that Spm^{4+} ions are located mostly in the regions of high negative potential density in the minor groove protecting the deoxyribose ring from this side against radiolytic degradation (Sy et al., 1999).

Below we describe the result of analysis of the MD computer simulations for the Spm/Na, Na-3DNA, and Na-1DNA systems with focus on the DNA hydration, Na$^+$-DNA interactions, and analyzing the interplay between the DNA structure and Na$^+$/Spm^{4+}/water competition for binding to the DNA.

TABLE 3 Averaged occupancies and residence times (in ps) for water, sodium, and charged nitrogen atoms of spermine

	O$_{H2O}$	Na$^+$	N$^+_{terminal}$	N$^+_{central}$
Phosphate oxygen				
O1P				
Occupancy	2.62/2.97	0.04/0.15	0.08	0.045
Residence time	5.4/5.2	25/28	22	15
O2P				
Occupancy	2.68/2.79	0.04/0.056	0.06	0.02
Residence time	6.4/7.2	25/15	10	8.4
Minor groove				
T$_{O2}$				
Occupancy	1.07/1.30	0.07/0.02	0.04	0.05
Residence time	4.2/5.1	130/29	22	6.1
C$_{O2}$				
Occupancy	0.80/1.13	0.002/0.035	0.08	0.03
Residence time	4.8/5.0	2.5/11.8	2.0	2.0
A$_{N3}$				
Occupancy	0.94/1.21	0.005/0.036	–	0.007
Residence time	7.5/5.6	5.7/5.9	–	1.4
G$_{N3}$				
Occupancy	1.04/1.24	0.004/0.000	0.01	–
Residence time	7.7/7.1	7.0/–	2.4	–
Major groove				
A$_{N7}$				
Occupancy	1.20/–	0.033/0.20	0.013	0.003
Residence time	3.85/–	20.8/16.0	3.0	1.7
G$_{N7}$				
Occupancy	1.31/1.07	0.04/0.30	0	–
Residence time	4.4/5.0	30/63	0.3	–
G$_{O6}$				
Occupancy	1.49/–	0.07/0.29	–	–
Residence time	4.9/–	20.5/72	–	–
T$_{O4}$				
Occupancy	1.06/1.11	0.02/0.089	–	–
Residence time	4.5/4.9	10.9/9.1	–	–
Sugar				
O4*				
Occupancy	1.00/1.25	0.01/0.023	0.034	0.018
Residence time	3.7/3.8	8.2/12.0	4.1	2.5

For the data separated by a slash, the first figure reports the value obtained in the Spm/Na system, the second one is for the Na-3DNA system.

CA/TG fragment

A CA/TG fragment is repeated three times in each decamer. We have therefore chosen this fragment for a more detailed analysis because this particular sequence allows the collection of the most reliable statistics on interactions between the mobile species and the DNA atoms. We have determined the averaged structures of the CA/TG fragment and spatial distribution functions of the surrounding species in all three MD simulations that we discuss in this work. The averaged DNA structures and SDFs are shown in Fig. 2, *A* and *C* for the Spm/Na simulation; the results obtained in the Na-3DNA simulation are displayed in Fig. 2, *B* and *D*. The averaged structures of the CA/TG fragment are similar for all three MD simulations; RMS deviations calculated for the heavy DNA atoms, are in the range of 0.45 to 0.65 Å. The

major part of the RMS difference originates from the orientation and positions of the phosphate groups, whereas the coordinates of the bases coincide very well.

In averaging the distribution of waters and ions between the three CA/TG fragments in the DNA decamer, we have enhanced the features inherent to all such two-base fragments. On the other hand, features depending on the long-range elements of the DNA structure, i.e., on the neighboring bases, become smeared out. For example, in the major groove, the water binding to DNA depends on the long-range sequence-specific "mosaic" structure of the H bond donors and acceptors. This explains why the details of water structure in the major grove are not visible in Fig. 2, whereas they become visible in the SDF drawn around the whole decamer (see below in Figs. 3–6).

As it can be seen from the data presented in Tables 2 and 3, water molecules interact most frequently with the phosphate groups. The intensity of the first maximum of the RDF for the oxygen atom near the phosphates O1P and O2P, is 3 to 5 times higher than those calculated for sites at the DNA bases. A part of this difference comes from the larger "available volume" around the phosphate oxygens pointing out from the backbone and which are exposed to water and have more free space around them than the atoms of the bases, which are surrounded, by atoms of other stacked bases. It is hard to expect that this effect contributes more than a factor of 2 in the RDF intensity difference. In accordance with x-ray diffraction and other MD simulation studies (Schneider et al., 1998; Duan et al., 1997; Feig and Pettitt, 1999b; Lyubartsev and Laaksonen, 1998), the binding of water to the phosphate groups is delocalized in space with each phosphate group being coordinated by approximately 3 water molecules (Table 3; Fig. 2). By decreasing the intensity threshold for the SDFs of water, it is possible to see the second diffuse spherical solvation shells around each PO$_4^-$ group (not shown in Fig. 2).

For the minor groove of the CA/TG fragment, several high concentration regions of ordered water molecules can be seen. These water maxima correlate reasonably well with the positions determined by statistical analysis of x-ray crystallography data for the hydration sites around bases in the B-form of DNA (Schneider and Berman, 1995) (shown as small magenta spheres in Fig. 2, *A* and *B*). Hydration sites of A$_{N3}$, C$_{O2}$, and two of the three minor groove hydration sites of the guanine base obtained in the MD simulations are close to those obtained from this analysis. Some specific locations of hydration water are so well defined that it is possible to see "images" of water molecules, formed by water oxygen and hydrogen SDF (encircled in Fig. 2 *A* and also in Fig. 2 *B*). An example of this is in the top right corner of Fig. 3 *A*, where a water molecule is seen near T$_{O2}$, shifted somewhat closer to the sugar ring as compared with the analysis of Schneider and Berman (1995).

There are several regions in the minor groove where sodium ions and charged amino groups of spermine can be

TABLE 4 Selected sites of DNA bases for binding of Na$^+$

DNA site	RDF(I)	Occup.	Res. time	Neigh. Site	RDF(II)
Minor groove					
T2$_{O2}$	9.5/0.0 (2.3)	0.133/0.0	94/0 (1800/0)	T19$_{O2}$	11.0/0 (2.3)
				A1$_{N3}$	3.2/0.7 (4.7)
T19$_{O2}$	11.0/0.0 (2.3)	0.157/0	127/0 (2000/0)	T2$_{O2}$	9.5/0 (2.3)
				A18$_{N3}$	1.3/0.55 (5.3)
T11$_{O2}$	3.6/0.5 (2.3)	0.046/0.023	126/18 (900/110)	G10$_{N3}$	1.6/0 (4.8)
C20$_{O2}$	3.5/0.7 (4.4)	–	–	A1$_{N3}$	3.2/0.7 (4.7)
				T19$_{O2}$	0.9/1.4 (4.6)
Major groove					
G10$_{N7}$	23/23 (2.4)	0.30/0.66	150/95 (2100/1400)	G10$_{O6}$	14/21 (2.4)
				A9$_{N7}$	7.0/12.5 (2.6)
				T19$_{O4}$	2.3/2.7 (4.3)
G6$_{N7}$	8.5/28 (2.4)	0.17/0.72	49/320 (900/1400)	G6$_{O6}$	0.2/15 (2.4)
				T7$_{O4}$	0.8/2.3 (4.3)
				A5$_{N7}$	4.5/6.5 (2.6)
				A5$_{O2P}$	–
A1$_{N7}$	0.85/0.4 (2.5)	0.018/0.017	53/6 (300/150)	–	–
T2$_{O4}$	1.5/0.3 (2.4)	0.034/0.016	6.9/8.8 (270/90)	G3$_{O6}$	8.5/1.1 (2.4)
A5$_{N7}$	4.5/6.5 (2.5)	0.002/0.40	6.9/7.7 (24/400)	G6$_{O6}$	1.9/0.8 (4.7)
				G6$_{N7}$	1.0/1.0 (4.5)
T7$_{O4}$	3.4/9.0 (2.3)	0.053/0.38	100 (400)	G12$_{O6}$	2.4/0.3 (2.3)

RDF(I), The intensity of the first maximum and the corresponding position in Å (in parenthesis); Occup., occupation (coordination) number; Res. time, average residence time in ps (rounded longest observed time given in parenthesis); Neigh. Site, nearest neighboring site; RDF(II), RDF information from the neighboring site, relative intensity and position of the maximum in Å (in parenthesis).

For the data separated by a slash, the first figure reports the value obtained in the Spm/Na system, the second one is for the Na-3DNA system.

localized inside the first hydration layer of DNA. This can be seen particularly well in Fig. 2 *C* displaying a view of Fig. 2 *A* from the bottom, perpendicular to the helix axis, with an isodensity threshold value of the SDFs for these ions that is one-half of that used in Fig. 2 *A*. To the right, i.e., in Fig. 2, *B* and *D*, the same result as that in Fig. 2, *A* and *C*, is now displayed for the Na-3DNA system. There exist certain similarities in spatial distributions of Na$^+$ and spermine ions. In the minor groove, a similarity in the distribution of Na$^+$ and N$^+$ of spermine becomes visible after lowering the threshold density from that used in Fig. 2, *A* and *B* by a factor of two. Fig. 2 *C* shows that a nearly continuous ribbon-like feature of cation (Na$^+$ and N$^+$ of spermine) density follows the path of the B-DNA minor groove. A similar continuous distribution of Na$^+$ ion was observed in the Na-1DNA system (Lyubartsev and Laaksonen, 1998). In the case of the Na-3DNA system, the maxima of the Na$^+$ density distribution are seen along the same path, though in this case they do not seem to form a clear unbroken density along the minor groove for the 5 p/nm^3 level (Fig. 2 *D*). In the minor groove, the hydration of the bases is regular both in the spermine containing and in the two pure sodium systems. Na$^+$ ions interact only occasionally with the bases directly, as can be seen in the RDFs (Tables 2 and 3) but not in the SDFs at the given threshold level. Instead, Na$^+$ ions organize the solvent structure and interact with the bases via water molecules.

Another difference between the three simulations concerns the major groove. As we have mentioned earlier,

spermine molecules are not present in the major grove. As for Na$^+$ ions, we found quite a strong binding of Na$^+$ ions to N6 and O6 of guanine and N7 of adenine. For the Na-3DNA system this binding is noticeably stronger than in the case of the Spm/Na system (see Table 2) and also more pronounced than in the previous Na-1DNA simulations. Below, interaction of Na$^+$ with sites in the major groove will be discussed in more detail.

Decamer: hydration and ion association

Fig. 3 illustrates and compares the potential of the x-ray crystallography and MD simulation methods in describing DNA hydration and ligand interactions. The figure compares the coordination of water and ions determined in the x-ray work of Shui et al. (1998b) (Fig. 3 *A*) with the results obtained for Spm/Na (Fig. 3 *B*) and Na-3DNA (Fig. 3 *C*) systems. The ordered positions of the water molecules in Fig. 3 *A* represent only a fraction of all species present in the DNA crystal and cannot be quantitatively compared with the SDFs in Fig. 3, *B* and *C*. The problem of distinguishing between solvent molecules and other substances, absorbed in the DNA crystal (mainly counterions), is a major challenge in the interpretation of electron density maps. Spatial distribution functions, on the other hand, calculated in the MD simulations can provide a detailed description of the DNA hydration and interactions with ligands (Beveridge and McConnell, 2000), nicely complementing the x-ray studies.
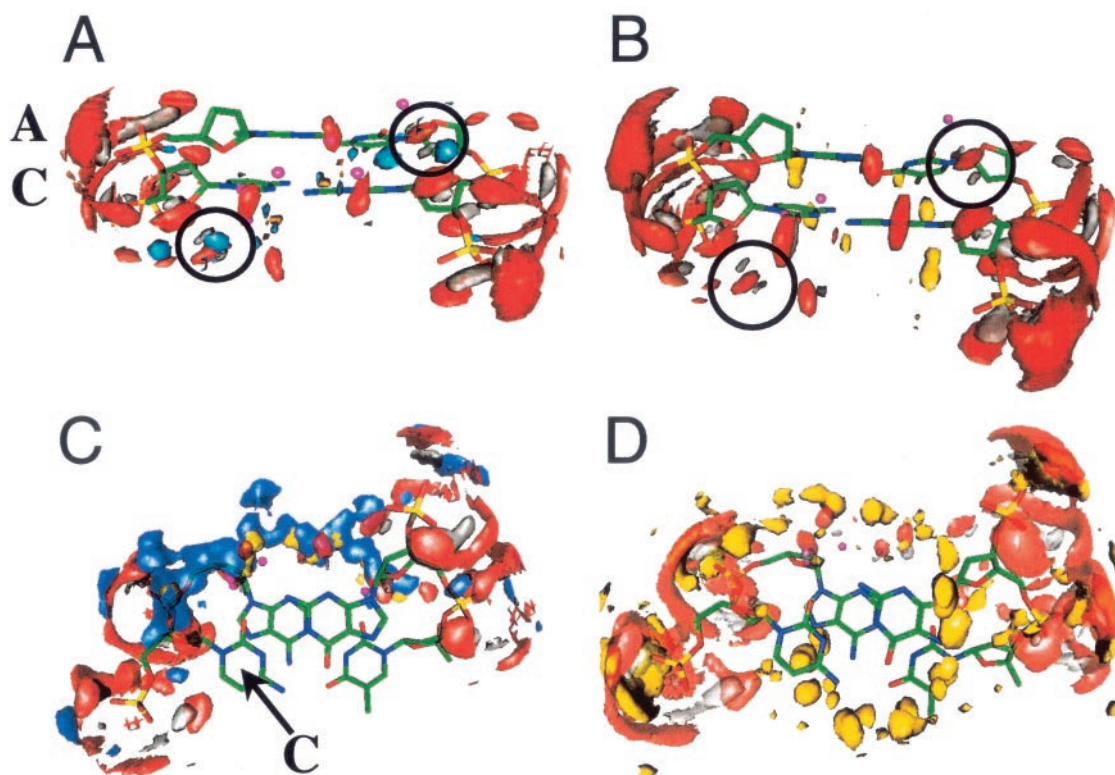
FIGURE 2 Averaged SDF of water and ions calculated for the CA/TG base pair step: (*A* and *C*) (*left panel*) Spm/Na system; (*B* and *D*) (*right panel*) Na-3DNA system. (*A* and *B*) Front view of the minor groove. (*C* and *D*) View along the helix axis seen from the bottom of Fig. 2, *A* or *B*. SDFs of water oxygen (*red*) and hydrogen (*gray*) atoms are drawn for density higher than 66 particles/nm^3 (p/nm^3); SDF of Na$^+$ ions (*yellow*) and/or N$^+$ atoms of spermine (*light blue*) are shown for density higher than 10 (*A* and *B*) or 5 p/nm^3 (*C* and *D*). (Density of pure water is ~33 p/nm^3). The hydration sites of the DNA bases in the minor groove calculated from x-ray crystallography data summarized by Schneider and Berman (1995) are drawn as small magenta spheres. Encircled are the "images" of water molecules at the positions of stable sequence-independent hydration in the minor groove.

Examination of the SDF images and the RDF curves of water molecules near the entire DNA decamer shows a reasonable agreement with x-ray crystallography data from different studies (Schneider and Berman, 1995; Schneider et al., 1998) and with previous MD simulations (Young et al., 1997; Duan et al., 1997; Feig and Pettitt, 1999a; Lyubartsev and Laaksonen, 1998). At the same time, some DNA hydration sites found in x-ray diffraction work have no analogous maxima in the SDFs of water oxygens, obtained in the MD simulations. This can be due to the dependence of the water structure in the minor and major grooves both on the DNA sequence and on the local geometry of DNA grooves. For example, the major groove of an (AATT)$_2$ fragment in the well-studied DDD duplex is wider than in sequences of alternating A/T and G/C base pairs. Another reason for the differences between the MD simulation of the spermine system, and x-ray diffraction studies may be due to the influence of crystal packing geometry. The MD simulation was performed in a hexagonal cell, whereas the most of B-form DNA crystals fit in an orthogonal lattice.

It is of interest to compare the hydration pattern obtained in the spermine system with that shown in Fig. 3 *C*, displaying the result from sodium system. The SDFs in Fig. 3,

B and *C* have been calculated with the same threshold values. The system with no spermine shows stronger hydration pattern caused by a more pronounced ordering of water assisted by the sodium ions. Feig and Pettitt (1998) also noted this influence of the sodium counterions on the water.

A more reliable quantitative display of hydration of the DNA groups can be obtained from the water occupancies obtained from the RDFs and occupancies values (listed in Tables 2 and 3), because the value of the spatial distribution function is dependent both on species density and on variation of DNA structure. This means that averaging of the DNA structure both in time and over 3 decamers in the simulation cell results in "smearing out" of the SDF due to dispersion in DNA coordinates. We have found that the DNA structure shows somewhat more flexibility in the Na-3DNA simulation than in the Spm/Na system. However, although the averaged structure of the DNA decamer in the Na-3DNA system shows higher RMS deviations for each atom than does the corresponding averaged structure of the Spm/Na simulation, one can still see that the SDF of the water oxygens is more defined and better structured around Na-DNA (Fig. 3 *C*) than in the mixed Spm/Na system (Fig.
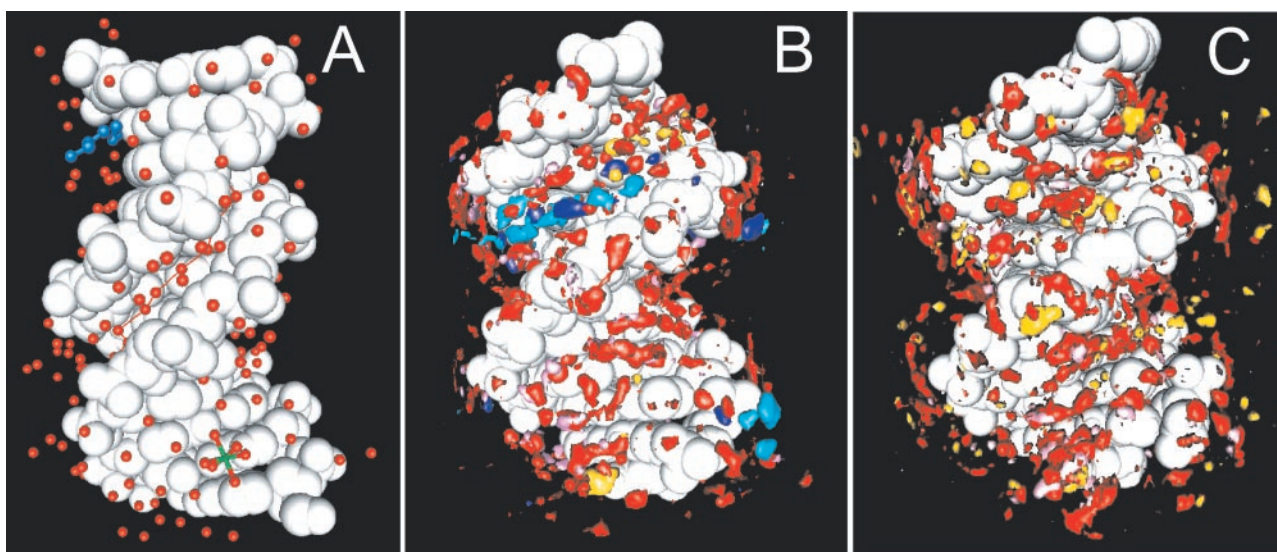
FIGURE 3   Comparison of the x-ray crystallography and MD simulation methods in interactions of DNA with water and ions. (*A*) x-ray crystallography data (DDD double helix, NDB, and PDB entry code BDL084 (Shui et al., 1998b)). Peaks of electron density assigned to water molecules (*red*), one spermine^{4+} fragment (*blue*), and one Mg^{2+} ion (*green*, with six coordinated water molecules) are shown as small spheres. Solvent molecules of the "spine of hydration" in the narrow minor groove of $(AATT)_2$ step are connected. MD simulations results of (*B*) Spm/Na system (this work) and (*C*) Na-3DNA system. Averaged SDFs of oxygen (*red*) and hydrogen (*pink*) water atoms are drawn for density higher than 66 p/nm^3; Na^+ (*yellow*) and N^+-atoms of spermine (*dark* and *light blue* colors are respectively for terminal and central nitrogen atoms) are shown for density higher than 17 (*B*) and 33 (*C*) p/nm^3. SDFs of Cl^- ions and of spermine carbon and hydrogen atoms are not shown.

3 *B*). Spermine, with a substantial fraction of hydrophobic methylene groups, excludes water molecules from the region it occupies and generally disrupts the hydration structure. The values of occupancies (Table 3), which are obtained by integrating the RDFs, clearly shows this more pronounced hydration of the Na-3DNA system, particularly in the minor groove, as compared with the Spm/Na system. In this context it should be noted that the values of the maxima of the intensity in the RDFs given in Table 2 is not a reliable measure for comparison of the extent of hydration between the different systems. First, the RDF values have been obtained relative to the mean concentration of particles in the simulation cell, and this leads to the absolute densities for Na^+ being two times lower for the Spm/Na system compared with the Na-3DNA system because the number of sodium ions in the latter system is two times higher than in the former one. Second, the larger amplitude of fluctuation of DNA coordinates in the Na-3DNA system (as compared with the Spm/Na system) results in broader RDF peaks. The destructive effect on the DNA hydration caused by the presence of spermine is also clearly seen in the analysis of site-specific interactions discussed below.

Water and ion coordination in the hydration shells of DNA bases

Our data support the results from other MD simulations and several NMR experiments showing evidence that water and monovalent cations share their occupancy at hydration positions of DNA bases. The RDF peak positions, their intensities, occupancies, and residence times of H_2O and Na^+ are listed in the first two columns in Tables 2 and 3. These values are obtained by averaging the trajectories of Na^+ and water over all the three decamers in the simulation cell, each decamer containing 20 oxygen atoms (O1P, O2P, and O4*), as well as the five atoms in each hydration site of the bases. Any sequence specific information tends to become lost in an averaging over the whole DNA system. To describe the site-specific (sequence-dependent) binding of Na^+ to DNA bases we have carried out a special separate analysis, summarized in Table 4. Figs. 4, 5, and 6 illustrate some examples of the site-specific distribution of Na^+, H_2O, and subgroups of Spm^{4+} around the decamer.

It can be seen that inside the first solvation shell around DNA the sodium ions can be found at positions of practically every electronegative group of the simulated decamer (Tables 2 and 3). However, the occupancies of each of the positions are strongly dependent on the nature of the particular site and also on the possibilities to coordinate to neighboring groups and water molecules (Table 4). Both Na^+ and H_2O are present around the phosphate groups. Although the intensity of the first maximum in the RDF of H_2O and Na^+ with O1P and O2P atoms are approximately equal (with the exception of the Na-O1P site in the Na-3DNA system), the absolute concentration of Na^+, expressed either as occupancy or in moles or number of particles per unit volume, comprises only ~2% of the corresponding value for O atoms of water (Tables 2 and 3).
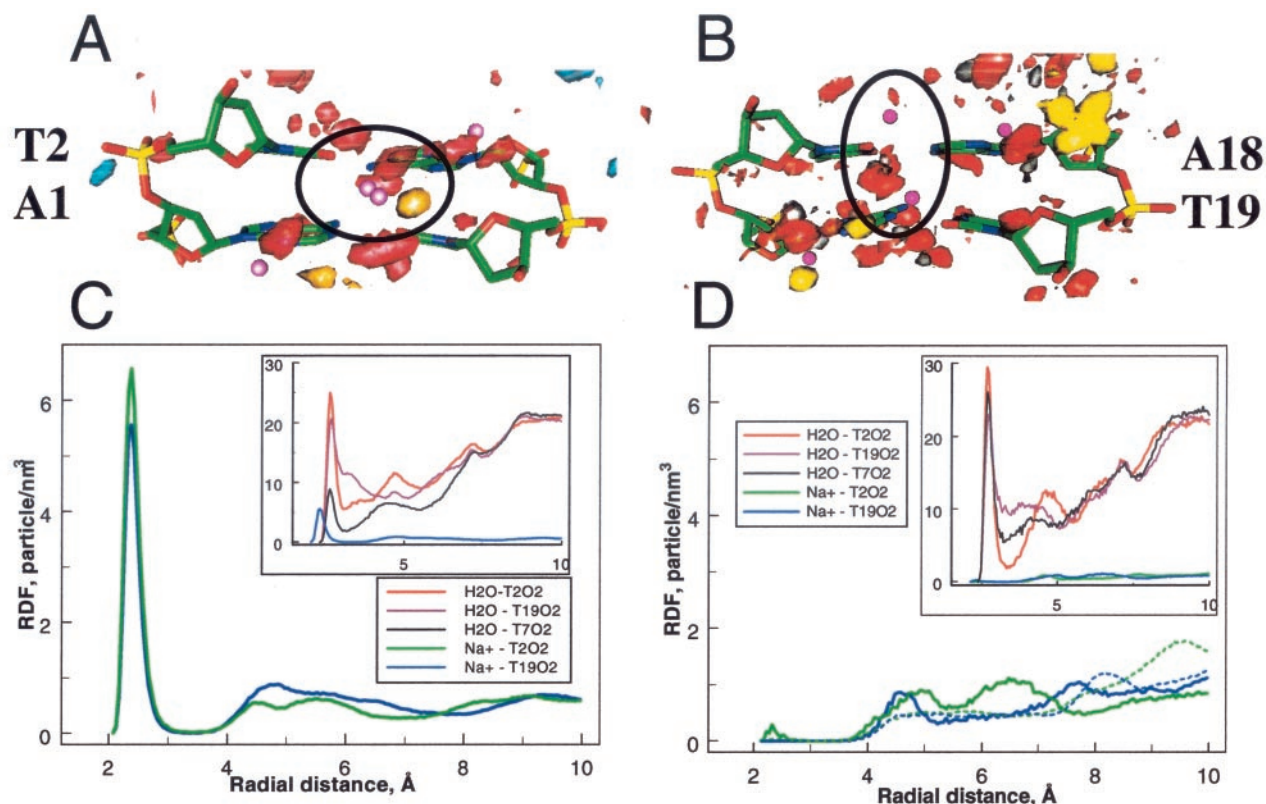
FIGURE 4   Binding of Na⁺ ions in the minor groove of the A1T2/A18T19 fragment. (*A* and *C*) (*left panel*) Spm/Na system (this work); (*B* and *D*) (*right panel*) Na-1DNA. (*A* and *B*) Averaged structure of DNA and SDFs of water oxygen (*red*; density higher than 100 p/nm³), Na⁺ (*yellow*; density higher than 50 (*A*) or 25 (*B*) p/nm³), and N⁺ of spermine (*blue*; density higher than 25 p/nm³). Central region of the minor groove is encircled. The hydration sites of DNA bases calculated from x-ray crystallography data summarized by (Schneider and Berman, 1995) are drawn as small magenta spheres. (*C* and *D*) RDFs of Na⁺ and water oxygen around T_{O2}-atoms. To compare the populations of water and Na⁺ near the DNA sites, RDFs were normalized relative to the corresponding mean particle density in the simulation cell. In the major graphs, Na⁺ coordination with $T2_{O2}$ (*green*) and $T19_{O2}$ (*blue*) is shown; in graph *D*, solid lines are for the Na-1DNA system, dotted ones is for Na-3DNA simulation. In the inserts of graphs *C* and *D*, the RDFs of Na⁺ are compared with the distribution of water oxygen near $T2_{O2}$ (*red*), $T19_{O2}$ (*magenta*), and $T8_{O2}$ (*black*).

The large number of Na⁺-OP contacts makes the averaged results of Na⁺-phosphate interactions statistically significant. Whereas the water molecules are distributed evenly between the O1P and O2P atoms, the Na⁺ and charged nitrogen atoms of Spm⁴⁺ show a preference to O1P over O2P because the distribution of O1P-atoms in the B form of DNA creates a region of negative electrostatic potential around the minor groove. The preferential Na⁺ and N⁺-atom binding to O1P over O2P is relatively small in the Spm/Na as well as in the Na-1DNA systems. The effect is more pronounced in the Na-3DNA simulation (Tables 2 and 3, data for Na-1DNA not shown). We believe that it may be related to a more significant binding of Na⁺ to the major groove of the Na-3DNA system. One possible consequence of the presence of Na⁺ in the major groove is that these Na⁺ ions induce rearrangement in the ion distribution on the opposite side of DNA double helix, in the minor groove. This would cause Na⁺ ions to be repelled further from the bottom of the minor groove, closer to the O1P-atoms. This may explain the absence of Na⁺ binding in the Na-3DNA

system at the highly electronegative site of the $T2_{O2}/T19_{O2}$ base pair (see discussions below regarding specific binding in the minor and major grooves).

Exchange of water molecules near the phosphate groups appears to be 4 to 5 times faster than that of Na⁺ ions and 2 to 4 times faster than for spermine N⁺ atoms (Table 3). Coordination of H₂O, Na⁺, and N⁺ with oxygen atom in the deoxyribose ring (O4*) is relatively weak, indicating that it may only serve as a secondary site in creation of the hydrogen bond network around DNA.

In the Spm/Na system the averaged water binding to specific hydration sites on DNA bases is relatively uniform (roughly one molecule per site), being weakest in the case of carbonyl oxygen of cytosine (with a coordination number of ~0.80) and strongest in the major groove with the amino group of cytosine and with O6 and N7 of guanine (~1.5 molecules/site; see Tables 2 and 3). In the Na-3DNA system, the hydration of the DNA bases (especially in the minor groove) is systematically higher than that in the Spm/Na system (Tables 2 and 3). Note that some occupancy
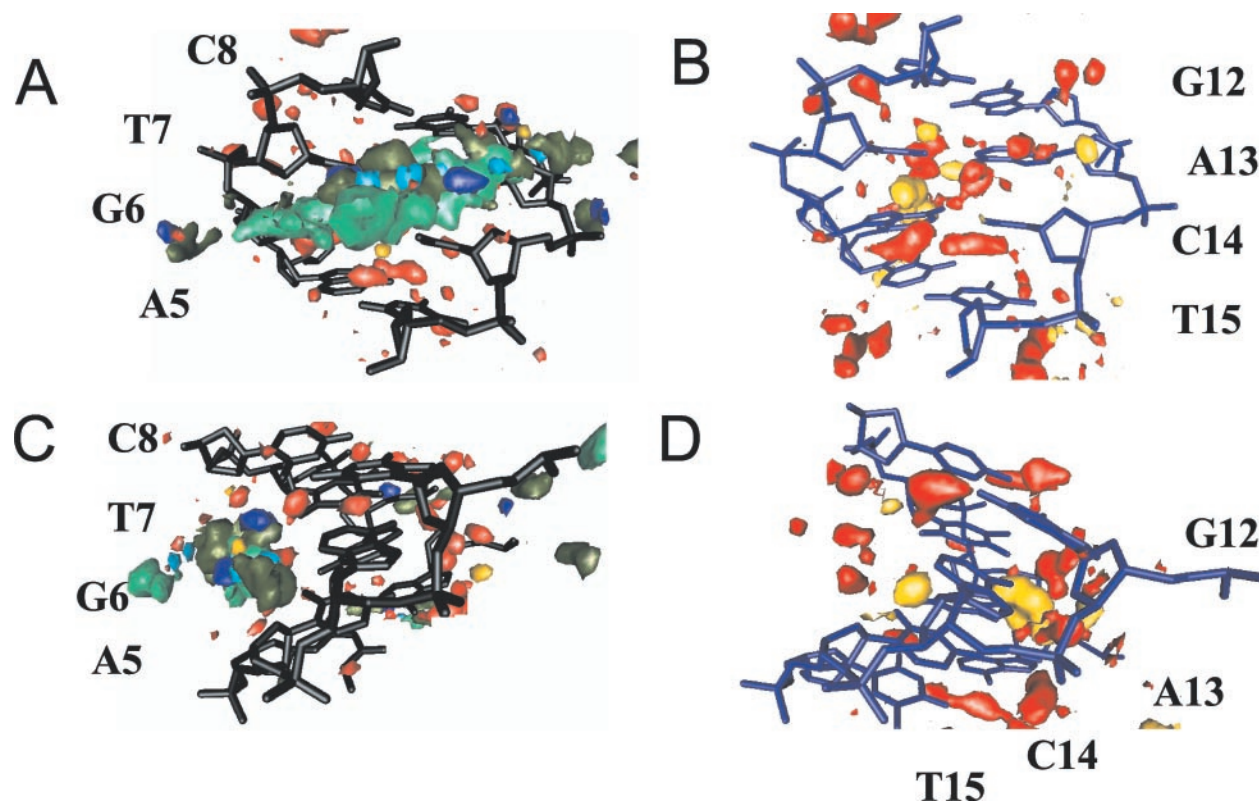
FIGURE 5   Region of spermine preferential binding in the minor groove of the DNA decamer (A5-C8/G12-T15). (*A* and *C*) (*left panel*) Spm/Na system; (*B* and *D*) (*right panel*) Na-3DNA system. (*A* and *B*) Front views of the minor groove; (*C* and *D*) view along the DNA minor groove. Colors and SDF threshold densities are chosen as follows: Na^+, yellow (30 p/nm^3); terminal and central N^+ of spermine, dark and light blue correspondingly (30 p/nm^3); $(CH_2)_3$ and $(CH_2)_4$ groups of spermine as dark and light green correspondingly (30 p/nm^3); oxygen atoms of water are in red for density higher than 100 p/nm^3.

values in Table 3 for the major groove sites in Na-3DNA could not be calculated due to the poor resolution between the first and second maxima in the RDF curves. The presence of Na^+ ions near the binding sites of the DNA bases varies substantially depending both on the nature of the site (Tables 2 and 3) and on its close neighborhood (Table 4). The Na^+ binding to specific sites and how this is influenced by the presence of spermine will be further discussed below.

Na^+ in the minor groove

In the minor groove of the Spm/Na system, the principal binding site for Na^+ ions is the carbonyl group of thymine. Most of the Na^+ binding to T_{O2} occurs at one specific site in the middle of the minor groove of the A1T2/A18T19 fragment (Table 4). The structure of this DNA fragment with SDFs is shown in Fig. 4 *A* together with RDFs (Fig. 4 *C*) of Na^+, water oxygen, and spermine N^+ atoms. To the right, Fig. 4, *B* and *D* show the corresponding results obtained from a similar analysis of this fragment of our previous Na-1DNA simulation (not Na-3DNA as in the rest of the figures). We have chosen to display the results from this simulation because we want to emphasize the effect on

the local DNA structure at this site, which is observed for both the Spm/Na and the Na-3DNA systems. In other respects such as sodium and water interaction the Na-1DNA and Na-3DNA systems show very similar behavior for this fragment. Comparison of the averaged structure of the A1T2/A18T19 fragment obtained in the simulation shows that this fragment in the Spm/Na system is very similar to that in the Na-3DNA system. The RMS deviation of the nonhydrogen atoms is only 0.36 Å. The A1/T19 and T2/A18 base pairs have a similar propeller twist (between $-12°$ and $-17°$) resulting in a "merging" of the hydration sites of the $T2_{O2}$ and $T19_{O2}$ oxygen atoms (shown as magenta spheres within the encircled area in Fig. 4 *A*). The distance between the two T_{O2} hydration sites is 0.56 and 0.36 Å for the Spm/Na and Na-3DNA systems, respectively. In contrast, the structure of the A1T2/A18T19 two-base-pair step in Na-1DNA differs from that found in Spm/Na and Na-3DNA, and this difference is mainly due to the absence of the negative propeller twist of the T2/A18 base pair. As a result of this, the separation between the $T2_{O2}$ and $T19_{O2}$ hydration sites is 3.22 Å (shown within the encircled area in Fig. 4 *B*). Therefore, in the Spm/Na and Na-3DNA systems, the T_{O2}-atoms are ideally arranged for coordination of a
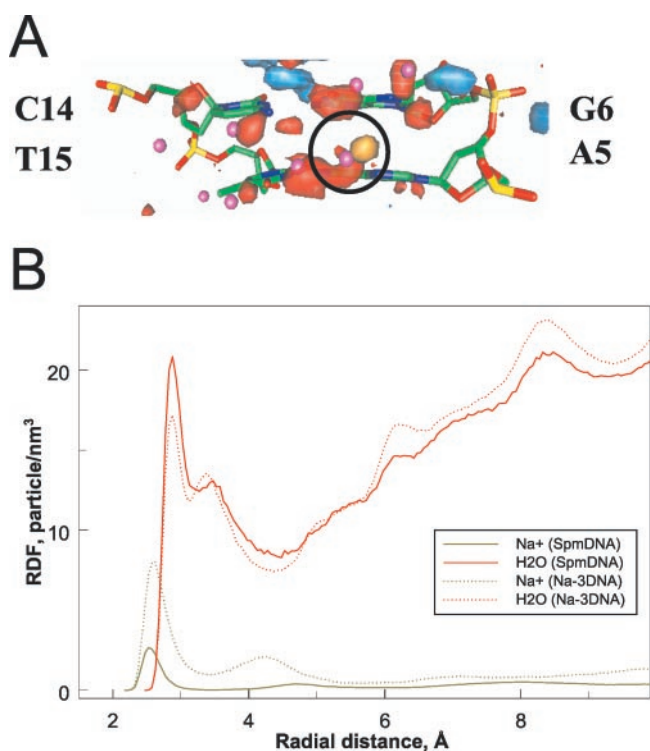
FIGURE 6 Binding of Na$^+$ in the major groove of the A5G6/C14T15 fragment. (*A*) Averaged structure of DNA and SDFs of water oxygen (*red*; density higher than 100 p/nm^3), Na$^+$ (*yellow*; density higher than 50 p/nm^3), and N$^+$ of spermine (*blue*; density higher than 25 p/nm^3) are shown. The region of Na$^+$ localization is encircled. The hydration sites of DNA bases calculated from x-ray crystallography data summarized by Schneider and Berman (1995) are drawn as small magenta spheres. (*B*) Normalized RDFs of Na$^+$ (*brown*) and water oxygen (*red*) around A5$_{N7}$ atom. Solid lines were obtained for the Spm/Na system; the dotted ones were determined from the MD simulation data in Na-3DNA system and drawn for comparison.

single water molecule or a Na$^+$ ion. A plausible explanation for this rather complex picture is that the hydration of DNA is a more important factor for modulation the local DNA structure than binding of Na$^+$ or Spm^{4+}. We suggest that merging of the two T$_{O2}$ hydration sites into one leads to a more economic hydration of DNA, which is important when the number of water molecules in the crystal is limited (the Na-3DNA and the Spm/Na systems contain 20 water molecules per nucleotide compared with 25 in the Na-1DNA system). Thus, the interaction between water and DNA should be a more powerful factor in modulation of the DNA structure than the transient presence of cations near the hydration sites. In this context it may be noted that experimental data point out a range between 20 and 25 H$_2$O/nucleotide as being critical for saturation of DNA hydration sites (Falk et al., 1962; Lee et al., 1987; Lindsay et al., 1988) as well as being important for the A-B transition in Na-DNA (Egli et al., 1998; Feig and Pettitt, 1998).

Interestingly, the presence of the electronegative cavity in the minor groove of the A1T2/A18T19 fragment in the Spm/Na and the Na-3DNA systems attracts sodium ions only in the case of the Spm/Na system. This can be seen from the RDFs of Na$^+$ to the T2$_{O2}$, T19$_{O2}$ atoms shown Fig. 4 *C* (Spm/Na system) and in Fig. 4 *D* shown as solid (Na-1DNA) and dotted (Na-3DNA) blue and green lines. This difference in sodium binding may be due to the fact that for the Spm/Na system, spermine molecules occupy the phosphate groups to a large extent and due to this competition, sodium ions go to the T2$_{O2}$/T19$_{O2}$ site, which in the Na-3DNA system is occupied by water molecules. As suggested above, the absence of sodium binding at this site in the Na-3DNA system may be due to the high Na$^+$ occupancy at the G10$_{N7}$-G10$_{O6}$ site on the opposite site of the major groove (Table 4; note that due to the periodicity along the z axis, a mirror image of the G10 nucleotide forms a base pair with a C20 nucleotide just below the A1/T19 base pair). The low dielectric constant of the DNA bases should increase this influence of the presence of Na$^+$ in the major groove on the electric field in the minor groove, thus reducing the negative potential at the T2$_{O2}$/T19$_{O2}$ site.

Fig. 4 *A* shows that the presence of Spm^{4+} around the A1T2/A18T19 fragment can only be seen at the periphery, near the PO$_4$-groups (in Fig. 4 *A*, the SDF of the N$^+$ atoms is shown in blue). However, the presence of Spm^{4+} in some other locations of the decamer minor groove (e.g., in the A5-C8/G12-T15 region) repels water molecules from the minor groove. This effect can be seen by comparing the H$_2$O-T7$_{O2}$ RDFs for the Spm/Na with those of the Na-3DNA/Na-1DNA systems (the black lines in the inserts of Fig. 4, *C* and *D*). The corresponding curve for the Na-3DNA system is very similar (data not shown).

The MD simulations show that the DNA double helix can change its conformation locally (as shown by the propeller twist of the T2 and T19 bases). It is of course possible that this change of the local DNA conformation may not reflect a real event but may be a consequence of an improper description of base stacking interactions in the force field parameters or does not represent statistically averaged conformations due to a short simulation time. In the center of the (AATT)$_2$ fragment of the DDD duplex, the narrowing of the minor groove also results in merging of hydration sites of the bases and provides an optimal distance for coordination of water or Na$^+$ with the two T$_{O2}$-atoms of opposite DNA strands. In agreement with the present work, x-ray diffraction, NMR relaxation, and MD simulations studies of the DDD duplex point to the central position in the minor groove "spine of hydration" as a location where partial substitution of water by cations can take place (Shui et al., 1998a,b; Sines et al., 2000; Denisov and Halle, 2000; Tereshko et al., 1999a,b; Hamelberg et al., 2000; McConnell and Beveridge, 2000).

Effect of spermine on hydration of the minor groove

Fig. 5 compares the averaged DNA structure and SDFs obtained for the decamer fragment A5-C8/G12-T15 in the MD simulations of the Spm/Na system (Fig. 5, A and C, left panel) and for the Na-3DNA system (Fig. 5, B and D, right panel). The averaged DNA structures of the A5-C8/G12-T15 fragment are similar for all the three systems we have studied (the RMS difference is between 0.4–0.8 Å). The positions and densities of the cationic species are also similar. However, the presence of the spermine methylene groups illustrated by the SDFs of the carbon atoms in the $(CH2)_3$ and $(CH2)_4$ groups (shown respectively as dark and light green), makes a decisive influence on the minor groove hydration of the fragment. The hydrophobic methylene groups of spermine push water out of the groove, whereas Na^+ attracts and organizes water around DNA. Note that the SDF of the water oxygen atom (shown in red) in Fig. 5, B and D is more intense than in Fig. 5, A and C. The water O-atom RDF shown in Fig. 4, C and D also supports the explanation that the depletion of water in the minor groove is caused by the partly hydrophobic spermine. We can conclude that the Na^+ ions share their presence with water and form a number of water-mediated contacts with different groups of DNA, whereas the presence of the methylene groups of Spm^{4+} disrupts the water structure at this position in the minor groove.

Na^+ in the major groove

Several potential Na^+ binding positions to electronegative groups of DNA bases can be found in the major groove (Table 4, Fig. 6; see also Korolev et al., 2001). The strongest Na^+-base interactions are observed close to the guanine N7 and O6 atoms and the adenine N7 atom (Tables 2–4). This interaction increases in the series Spm/Na < Na-1DNA < Na-3DNA system. For the case of the Na-3DNA system, the binding of Na^+ to the G10 and G6 bases from the side of major groove is particularly strong (Table 4). As mentioned above this high Na^+ occupancy at the $G10_{N7}$ site of the Na-3DNA system is suggested to reduce the electronegative potential of the $T2_{O2}/T19_{O2}$ on the opposite site of the minor groove, contributing to the absence of sodium binding at that site.

As an example of Na^+ binding in the major groove, in Fig. 6 we have displayed SDF around the A5G6/C14T15 fragment of the Spm/Na system. The areas of high concentration of Na^+ and water coexist at this position. We have also included the SDFs of the N^+-atoms of Spm^{4+}, shown in light blue. The SDFs of water oxygens are in a reasonable agreement with the x-ray diffraction results, except for the two sites at the periphery of the major groove at C14 and T15 (Table 4).

Fig. 6 B illustrates the interaction of Na^+ with the DNA bases in the major groove of B-DNA. Na^+ ions coordinate with $G6_{N7}$ both in the Spm/Na and the Na-3DNA system (Table 4). This interaction is much stronger for the case of pure Na-DNA, as can be seen comparing the RDFs of the two systems (see also Tables 3 and 4, Fig. 2). Na^+ ions are capable to displace water from this position, which is manifested by a lower first maximum of the water RDF.

Our data on Na^+ binding to the bases in the major groove are in agreement with other MD results obtained for Na- (McConnell and Beveridge, 2000), K- (Auffinger and Westhof, 2001), Na-, and Cs-salts (Lyubartsev and Laaksonen, 1998) of DNA. Similar observations have recently been obtained in x-ray crystallography studies reporting the presence of Tl^+ ions coordinating with DNA bases in the major groove (Howerton et al., 2001).

Sodium ions also show several specific locations in the second solvation shell in the minor and major grooves of DNA. A closer analysis of Na^+ and water SDFs and RDFs shows that the presence of Na^+ increases the structuring of water. At the sites of strong Na^+ coordination, water molecules fill the positions around the Na^+ ions, forming a regular structure and extending the enhanced solvent network further away. Because we have not found any noticeable presence of spermine in the major groove of the decamer, this ligand cannot exert its destructive influence on water structure in this region.

Influence of cations on DNA structure

The ability of ions to directly and dynamically modulate DNA structure due to their presence near the DNA groups is a matter of debate in recent literature (Howerton et al., 2001; McFail-Isom et al., 1999; Hamelberg et al., 2000, 2001; Hud and Polak, 2001; McConnell and Beveridge, 2000 and references cited therein). Opinions range from the idea that even transient presence of ions (including monovalent cations) near the DNA molecule can immediately result in a change of the local DNA structure (McFail-Isom et al., 1999; Sines et al., 2000; Hamelberg et al., 2000, 2001) to a conception that such features of the DNA double helix as groove width or bending is dependent mostly on the base sequence and that only strongly bound, multivalent ions like Ca^{2+} or Mg^{2+} can change the DNA structure to a limited extent (Chiu and Dickerson, 2000; Chiu et al., 1999). The MD simulations reported in this work have the ambition to model the conditions of real DNA crystals and to allow comparison of our data with structural information obtained by mainly x-ray crystallography. In this section we discuss the influence of cations on DNA structure by analyzing the dependence of the width of DNA minor groove on the conditions of the DNA decamer surroundings. Analysis of trajectories from the Spm/Na and the Na-3DNA simulations shows that the width of the minor groove changes rather dynamically and quickly (on a subnanosecond time scale),
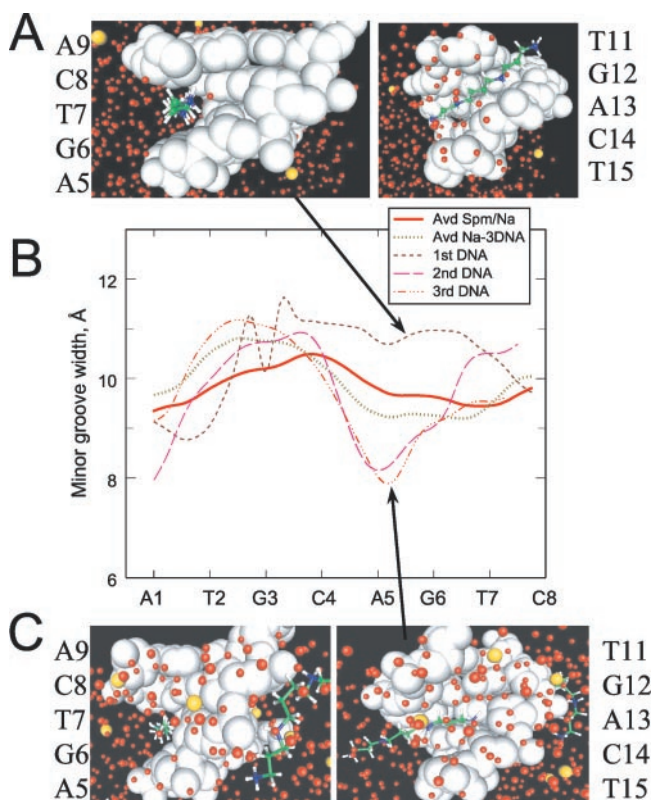
FIGURE 7 The width of the DNA minor groove and distribution of water and ions around DNA obtained in the Spm/Na system. (*B*) Change of the minor groove width along the DNA decamer. Thick lines are for averaged DNA structure obtained in Spm/Na (*solid*, *red*) and Na-3DNA (*dotted*, *brown*) systems. Thin lines are for the three DNA decamers in the simulation cell from a snapshot of the MD simulation at $t = 6.12$ ns. Program Curves 5.1 (Stofer and Lavery, 1994) was used to calculate DNA structural parameters. (*A* and *C*) Snapshot of the DNA structure (*gray-white space-filled presentation*) and distribution of spermine⁴⁺ (*sticks*), Na⁺ (*yellow spheres*), and oxygen atoms of water (*small, red spheres*) around the A5-A9/T11-T15 fragment in the DNA decamer for the first (*A*, *top*) and third (*C*, *bottom*) DNA molecules in the simulation cell. In *A* and *C*, right picture is front view of the minor groove; left picture is view along the minor groove from the top of the A5-A9/T11-T15 fragment.

in agreement with literature data (Hamelberg et al., 2000, 2001). The groove width is therefore useful for an analysis of the correlations between ion distribution and DNA structure. In Figs. 7 and 8 the change of the minor groove width along the DNA molecules is displayed for both the Spm/Na and the Na-3DNA systems. The data have been calculated using the Curves 5.1 program (Stofer and Lavery, 1994) from averaged DNA structures, as well as from snapshot structures of the three separate DNA decamers obtained from representative configurations. The examples presented in Figs. 7 and 8 show that no direct correlation can be observed between the groove width and the presence of Spm⁴⁺ or Na⁺ in or near the groove. In Fig. 7 it can be seen that Spm⁴⁺ is found at approximately the same position of the DNA decamer at the bottom of both a wide (Fig. 7 *A*) and a narrow (Fig. 7 *C*) minor groove segment. A similar
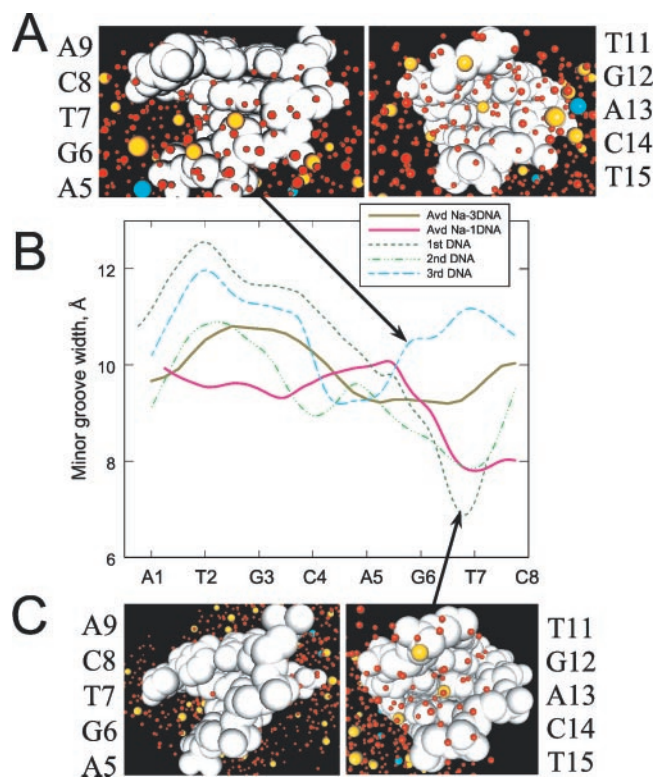

FIGURE 8 The width of the DNA minor groove and distribution of water and ions around DNA obtained in the Na-3DNA and the Na-1DNA systems. (*B*) Change of the minor groove width along the DNA decamer. Thick lines are for averaged DNA structure obtained in Na-3DNA (*brown*) and Na-1DNA (*magenta*) systems. Thin lines are for the three DNA decamers in the simulation cell from a snapshot of the Na-3DNA simulation run at $t = 3.2$ ns. (*A* and *C*) Around the A5-A9/T11-T15 fragment, ions of Na⁺ and Cl⁻ are shown as respectively yellow and cyan spheres, oxygen atoms of water are small, red spheres for the third (*A*, *top*) and first (*C*, *bottom*) DNA molecules in the simulation cell. Other details are as in Fig. 7.

picture is observed in the Na-3DNA system. Sodium ions can be found at the bottom or near the "lips" of the minor groove when it is both narrow (Fig. 8 *C*) and wide (Fig. 8 *A*). Our data are in good agreement with the results of the MD simulation study by (McConnell and Beveridge, 2000) reporting a rather indirect and complex response of the DNA structure to the presence of cations, which is contrary to the data by Hamelberg et al. (2000, 2001) advocating an instant and a rapid response of the DNA structure to the ionic environment.

Comparing the Spm/Na and Na-DNA systems, we did not find any straightforward correlation between the width of minor groove and the presence of spermine binding to DNA. The only difference between Spm/Na and Na-3DNA seen from the MD simulations is that Spm⁴⁺ reduces somewhat the amplitude of variation of the minor groove width. In Spm/Na, the width varies between 8 and 12 Å (Fig. 7 *B*, thin lines), and in Na-DNA the range of changes in the groove width is between 7 and 13 Å (Fig. 8 *B*, thin lines).

CONCLUSIONS

The possibility of M^+ ions to exchange water molecules in the first hydration shell of the DNA double helix and the ability of the mobile ions to modulate DNA structure has recently been debated in the literature. The main focus has been on the interpretation of results obtained in x-ray crystallography, NMR, and MD simulation studies of the cation/water dynamics inside the narrow minor groove of the $(AATT)_2$ fragment of the DDD duplex. In agreement with predictions from previous MD simulation studies our data confirm water/counterion exchange in the closest vicinity of DNA bases in general and near the thymine O_2-atoms in particular. In addition, we wish to underline that the extent of this exchange depends strongly not only on the nature of DNA binding site but also on the other parameters. In this context, we would also like to stress that the answer to the question about the presence of Na^+ (or other cations) in the first solvation shell of DNA bases is apparently rather complex. The extent of M^+/water exchange near each particular site depends on a wide number of structural parameters such as the DNA sequence, geometry of grooves, and on environmental factors such as the amount, and nature of ions in the crystal as well as activity of water.

Based on the MD simulation results, we can draw the following general conclusions. 1) Water molecules, Na^+ ions, and charged amino groups of spermine interact most frequently with the DNA phosphate groups. However, all these species form short-lived ion pairs with the charged O-atoms and the averaged distributions of the ligands around the phosphate groups of DNA are fairly diffuse. 2) Water is the principal molecule interacting with the DNA bases. The polar groups of DNA bases are hydrated in a uniform manner. 3) As a rule, water and ions form more stable long-lived pairs with the sites on DNA bases than near the phosphate groups. 4) Na^+ and amino groups of spermine can substitute water near the electronegative sites of the DNA bases. However, the extent of this substitution depends not only on the nature of the DNA group but is also a result of the structure of DNA in terms of availability and positions of other binding sites in the close vicinity. 5) The effect of the presence of the spermine molecule on the hydration and on the interaction of the sodium ions with DNA is significant. Spermine pushes water out of the minor groove while Na^+ attracts and organizes water around DNA. In the absence of spermine, with only sodium counterions, there is a larger hydration of DNA caused by substantial ordering of water. The hydrophobic methylene groups reduce the organization of water at the positions of spermine binding to DNA.

Specifically, concerning the B-DNA decamer studied in this work we can conclude that the mobile spermine molecules are highly present in the minor groove. As an example, it is found that amino groups of Spm^{4+} can be found for ~25% of the simulation time in the vicinity near the O_2

atom of the T7 base. In addition, based on comparison with analysis of the results of our previous work, we can also conclude that binding to DNA bases is very sensitive to the nature of the counterions (Lyubartsev and Laaksonen, 1998). Our simulations confirm results from previous MD and NMR studies concerning the presence of cations in the first solvation shell of DNA bases (McConnell and Beveridge, 2000; Williams and Maher, 2000 and references cited therein). Therefore, it is reasonable to conclude that in the DNA crystals, monovalent cations can substitute water in the first solvation shell when these ions are present in the crystals. However, the occupancies of the cations near the binding sites seem to be relatively small compared with that of water molecules.

Finally, as discussed in detail in our first presentation of the spermine simulation (Korolev et al., 2001), we note that the invisibility of spermine in x-ray diffraction studies is most likely caused by the fact that the highly flexible spermine molecules are not able to form structurally stable complexes with DNA. None of the modes of spermine binding, such as the formation of bridges between different DNA helices across major and minor grooves, as well binding in the minor groove, shows any clear regularity.

REFERENCES

Auffinger, P., and E. Westhof. 2001. Water and ion binding around $r(UpA)_{12}$ and $d(TpA)_{12}$ oligomers: comparison with RNA and DNA $(CpG)_{12}$ duplexes. *J. Mol. Biol.* 305:1057–1072.

Bancroft, D., L. D. Williams, A. Rich, and M. Egli. 1994. The low-temperature crystal structure of the pure-spermine form of Z-DNA reveals binding of a spermine molecule in the minor groove. *Biochemistry.* 33:1073–1086.

Beveridge, D. L., and K. J. McConnell. 2000. Nucleic acids: theory and computer simulation, Y2K. *Curr. Opin. Struct. Biol.* 10:182–196.

Bonvin, A. M. J. J. 2000. Localisation and dynamics of sodium counterions around DNA in solution from molecular dynamics simulations. *Eur. Biophys. J.* 29:57–60.

Cheathan, T. E., and P. A. Kollman. 1997. Molecular dynamics simulations highlight the structural differences among DNA:DNA, RNA:RNA, and DNA:RNA structures. *J. Am. Chem. Soc.* 119:4805–4825.

Chiu, T. K., and R. E. Dickerson. 2000. 1 Å crystal structures of B-DNA reveal sequence-specific binding and groove-specific bending of DNA by magnesium and calcium. *J. Mol. Biol.* 301:915–945.

Chiu, T. K., M. Kaczor-Grzeskowiak, and R. E. Dickerson. 1999. Absence of minor groove monovalent cations in the crosslinked dodecamer C-G-C-G-A-A-T-T-C-G-C-G. *J. Mol. Biol.* 292:589–608.

Cohen, S. L. 1998. A guide to the polyamines. Oxford University Press, New York, Oxford.

Cornell, W. D., R. Cieplak, C. L. Bayly, I. R. Gould, K. M. Merz, D. M. Ferguson, D. G. Spellmeyer, T. Fox, J. W. Caldwell, and P. A. Kollman. 1995. A second generation force field for the simulation of proteins, nucleic acids, and organic molecules. *J. Am. Chem. Soc.* 117: 5179–5197.

Deng, H., V. A. Bloomfield, J. M. Benevides, and G. J. Thomas. 2000. Structural basis of polyamine-DNA recognition: spermidine and sperm-

ine interactions with genomic B-DNAs of different GC content probed by Raman spectroscopy. *Nucleic Acids Res.* 28:3379–3385.

Denisov, V. P., and B. Halle. 2000. Sequence-specific binding of counterions to *B*-DNA. *Proc. Natl. Acad. Sci. U. S. A.* 97:629–633.

Drew, H. R., and R. E. Dickerson. 1981. Structure of a *B*-DNA dodecamer III. Geometry of hydration. *J. Mol. Biol.* 151:535–556.

Duan, Y., P. Wilkosz, M. Crowley, and J. M. Rosenberg. 1997. Molecular dynamics simulation study of DNA dodecamer d(CGCGAATTCGCG) in solution: conformation and hydration. *J. Mol. Biol.* 272:553–572.

Egli, M., V. Tereshko, M. Teplova, G. Minasov, A. Joachimiak, R. Sanishvili, C. M. Weeks, R. Miller, M. A. Maier, H. An, P. D. Cook, and M. Manoharan. 1998. X-ray crystallographic analysis of the hydration of A- and B-form DNA at atomic resolution. *Biopolymers.* 48:234–252.

Falk, M., K. A. Hartman, and R. C. Lord. 1962. Hydration of deoxyribonucleic acid. I. A gravimetric study. *J. Am. Chem. Soc.* 84:3843–3846.

Feig, M., and B. M. Pettitt. 1998. A molecular simulation picture of DNA hydration around A- and B-DNA. *Biopolymers.* 48:199–209.

Feig, M., and B. M. Pettitt. 1999a. Sodium and chlorine ions as part of the DNA solvation shell. *Biophys. J.* 77:1769–1781.

Feig, M., and B. M. Pettitt. 1999b. Modeling high resolution hydration patterns in correlation with DNA sequence and conformation. *J. Mol. Biol.* 286:1075–1095.

Feuerstein, B. G., N. Pattabiraman, and L. J. Marton. 1986. Spermine-DNA interactions: a theoretical study. *Proc. Natl. Acad. Sci. U. S. A.* 83:5948–5952.

Feuerstein, B. G., N. Pattabiraman, and L. J. Marton. 1990. Molecular mechanics of the interactions of spermine with DNA: DNA bending as a result of ligand binding. *Nucleic Acids Res.* 18:1271–1282.

Halle, B., and V. P. Denisov. 1998. Water and monovalent ions in the minor groove of B-DNA oligonucleotides as seen by NMR. *Biopolymers.* 48:210–233.

Hamelberg, D., L. McFail-Isom, L. D. Williams, and W. D. Wilson. 2000. Flexible structure of DNA: ion dependence of minor-groove structure and dynamics. *J. Am. Chem. Soc.* 122:10513–10520.

Hamelberg, D., L. D. Williams, and W. D. Wilson. 2001. Influence of the dynamic positions of cations on the structure of the DNA minor groove: sequence-dependent effects. *J. Am. Chem. Soc.* 123:7745–7755.

Haworth, I. S., A. Rodger, and W. G. Richards. 1992. A molecular dynamics simulation of a polyamine-induced conformational change of DNA: a possible mechanism for the B to Z transition. *J. Biomol. Struct. Dyn.* 10:195–211.

Howerton, S. B., C. C. Sines, L. VanDerveer, and L. D. Williams. 2001. Locating monovalent cations in the grooves of B-DNA. *Biochemistry.* 40:10023–10031.

Hud, N. V., and M. Polak. 2001. DNA-cation interactions: the major and minor grooves are flexible ionophores. *Curr. Opin. Struct. Biol.* 11:293–301.

Hud, N. V., P. Schultze, V. Sklenár, and J. Feigon. 1999. Binding sites and dynamics of ammonium ions in the minor groove of DNA duplexes in solution and the origin of DNA A-tract bending. *J. Mol. Biol.* 286:651–660.

Korolev, N., A. P. Lyubartsev, L. Nordenskiöld, and A. Laaksonen. 2001. Spermine: an "invisible" component in the crystals of *B*-DNA. A grand canonical Monte Carlo and molecular dynamics simulation study. *J. Mol. Biol.* 308:907–917.

Lee, S. A., S. M. Lindsay, J. W. Powel, T. Weidlich, N. J. Tao, G. D. Lewen, and A. Rupprecht. 1987. A Brillouin scattering study of the hydration of Li- and Na-DNA films. *Biopolymers.* 26:1637–1665.

Lindsay, S. M., S. A. Lee, J. W. Powel, T. Weidlich, C. DeMarco, G. D. Lewen, N. J. Tao, and A. Rupprecht. 1988. The origin of the A to B transition in DNA fibers and films. *Biopolymers.* 27:1015–1043.

Lyubartsev, A. P., and A. Laaksonen. 1998. Molecular dynamics simulations of DNA in solution with different counter-ions. *J. Biomol. Struct. Dyn.* 16:579–592.

Lyubartsev, A. P., and A. Laaksonen. 1999. Effective potentials for ion-DNA interactions. *J. Chem. Phys.* 111:11207–11215.

Lyubartsev, A. P., and A. Laaksonen. 2000. M.Dyna*Mix* - a scalable portable parallel MD simulation package for arbitrary molecular mixtures. *Comp. Phys. Comm.* 128:565–589.

MacKerell, A. D., J. Wiorkiewiczkuczera, and M. Karplus. 1995. An all-atom empirical energy function for the simulation of nucleic-acids. *J. Am. Chem. Soc.* 117:11946–11975.

McConnell, K. J., and D. L. Beveridge. 2000. DNA structure: What's in charge? *J. Mol. Biol.* 304:803–820.

McFail-Isom, L., C. C. Sines, and L. D. Williams. 1999. DNA structure: cations in charge? *Curr. Opin. Struct. Biol.* 9:298–304.

Schneider, B., and H. M. Berman. 1995. Hydration of the DNA bases is local. *Biophys. J.* 69:2661–2669.

Schneider, B., K. Patel, and H. M. Berman. 1998. Hydration of the phosphate group in double-helical DNA. *Biophys. J.* 75:2422–2434.

Shamma, T., and I. S. Haworth. 1999. Spermine inhibition of the 2,5-diaziridinyl-1,4-benzoquinone (DZQ) crosslinking reaction with DNA duplexes containing poly(purine)-poly(pyrimidine) tracts. *Nucleic Acids Res.* 27:2601–2609.

Shui, X., L. McFail-Isom, G. G. Hu, and L. D. Williams. 1998b. The B-DNA dodecamer at high resolution reveals a spine of water on sodium. *Biochemistry.* 37:8341–8355.

Shui, X., C. C. Sines, L. McFail-Isom, L. VanDerveer, and L. D. Williams. 1998a. Structure of the potassium form of CGCGAATTCGCG: DNA deformation by electrostatic collapse around inorganic cations. *Biochemistry.* 37:16877–16887.

Sines, C. C., L. McFail-Isom, S. B. Howerton, L. VanDerveer, and L. D. Williams. 2000. Cations mediate B-DNA conformational heterogenity. *J. Am. Chem. Soc.* 122:11048–11056.

Soler-Lopez, M., L. Malinina, J. Liu, T. Huynh-Dinh, and J. A. Subirana. 1999. Water and ions in a high-resolution structure of B-DNA. *J. Biol. Chem.* 274:23683–23686.

Soler-Lopez, M., L. Malinina, and J. A. Subirana. 2000. Solvent organization in an oligonucleotide crystal: the structure of d(GCGAATTCG)$_2$ at atomic resolution. *J. Biol. Chem.* 275:23034–23044.

Stofer, E., and R. Lavery. 1994. Measuring the geometry of DNA grooves. *Biopolymers.* 34:337–346.

Sy, D., S. Hugot, C. Savoye, S. Ruiz, M. Charlier, and M. Spotheim-Maurizot. 1999. Radioprotection of DNA by spermine: a molecular modelling approach. *Int. J. Radiat. Biol.* 75:953–961.

Tereshko, V., G. Minasov, and M. Egli. 1999a. The Dickerson-Drew B-DNA dodecamer revisited at atomic resolution. *J. Am. Chem. Soc.* 121:470–471.

Tereshko, V., G. Minasov, and M. Egli. 1999b. A "hydrate-ion" spine in a B-DNA minor groove. *J. Am. Chem. Soc.* 121:3590–3595.

Tippin, D. B., and M. Sundaralingam. 1997. Nine polymorphic crystal structures of d(CCGGGCCCGG), d(CCGGGCCm^{5}CGG), d(Cm^{5}CGGGCCm^{5}CGG) and d(CCGGGCC(Br)^{5}CGG) in three different conformations: effects of spermine binding and methylation on the bending and condensation of *A*-DNA. *J. Mol. Biol.* 267:1171–1185.

Toukan, K., and A. Rahman. 1985. Molecular-dynamics study of atomic motions in water. *Phys. Rev. B.* 31:2643–2648.

Tuckerman, M., B. Berne, and G. J. Martyna. 1992. Reversible multiple time scale molecular-dynamics. *J. Chem. Phys.* 97:1990–2001.

Vlieghe, D., J. P. Turkenburg, and L. Van Meervelt. 1999. B-DNA at atomic resolution reveals extended hydration pattern. *Acta Cryst. Sect. D.* 55:1495–1502.

Williams, L. D., and J. L. Maher. 2000. Electrostatic mechanisms of DNA deformation. *Annu. Rev. Biophys. Biomol. Struct.* 29:497–521.

Young, M. A., G. Ravishanker, and D. L. Beveridge. 1997. A 5-nanosecond molecular dynamics trajectory for B-DNA: analysis of structure, motions, and solvation. *Biophys. J.* 73:2313–2336.

Yuki, M., V. Grukhin, C.-S. Lee, and I. S. Haworth. 1996. Spermine binding to GC-rich DNA: experimental and theoretical studies. *Arch. Biochem. Biophys.* 325:39–46.

Zakrzewska, K., and B. Pullman. 1986. Spermine-nucleic acid interactions: a theoretical study. *Biopolymers.* 25:375–392.